

Towards Quantum-Ready Blockchain Fraud Detection via Ensemble Graph Neural Networks

M.Z. Haider¹, Tayyaba Noreen¹, M. Salman²

¹Department of Software Engineering(ÉTS), Université du Québec, Canada

²Department of Computer Science, SZABIST University

Abstract—Blockchain Business applications and cryptocurrencies such as enable secure, decentralized value transfer, yet their pseudonymous nature creates opportunities for illicit activity, challenging regulators and exchanges in anti-money laundering (AML) enforcement. Detecting fraudulent transactions in blockchain networks requires models that can capture both structural and temporal dependencies while remaining resilient to noise, imbalance, and adversarial behavior. In this work, we propose an ensemble framework that integrates Graph Convolutional Networks (GCN), Graph Attention Networks (GAT), and Graph Isomorphism Networks (GIN) to enhance blockchain fraud detection. Using the real-world Elliptic dataset, our tuned soft voting ensemble achieves high recall of illicit transactions while maintaining a false positive rate below 1%, beating individual GNN models and baseline methods. The modular architecture incorporates quantum-ready design hooks, allowing seamless future integration of quantum feature mappings and hybrid quantum–classical graph neural networks. This ensures scalability, robustness, and long-term adaptability as quantum computing technologies mature. Our findings highlight ensemble GNNs as a practical and forward-looking solution for real-time cryptocurrency monitoring, providing both immediate AML utility and a pathway toward quantum-enhanced financial security analytics.

Index Terms—Blockchain Fraud Detection, Graph Neural Networks, Ensemble Learning, Quantum Machine Learning, Quantum-Ready Systems

I. INTRODUCTION

Blockchain has transformed digital finance by enabling secure, decentralized, and transparent transactions, with Bitcoin showcasing its global potential. Yet, the pseudonymous nature of cryptocurrency also facilitates illicit activities such as money laundering and ransomware, creating challenges for AML enforcement [1]. Detecting fraud is difficult due to the scale and complexity of blockchain transaction graphs, where conventional machine learning often falls short. Graph Neural Networks (GNNs) address this gap by capturing relational and structural patterns [2], [3]. While GCNs, GATs, and GINs each offer unique strengths, single models remain sensitive to noise and sparsity[4]. To overcome this, we propose an ensemble framework integrating these architectures via equal-weight, tuned-weight, and stacking strategies. The tuned soft-voting ensemble achieves the best results, detecting over 70% of illicit transactions in the Elliptic dataset with under 1% false positives, demonstrating practical value for real-time AML[1], [5].

Graph Neural Networks (GNNs) have advanced blockchain analytics beyond shallow embeddings and hand-crafted features by combining node attributes with multi-hop structural dependencies. Weber et al. [1] demonstrated the effectiveness of GCNs on the Bitcoin Elliptic dataset for AML tasks, while Wang et al. [3] showed that incorporating topological and temporal features further improves illicit transaction detection in large-scale networks. Similarly, Gai et al. [2] proposed a privacy-preserving federated GNN framework for financial data, supporting collaborative model training without exposing sensitive information[6]. Beyond classical GNNs such as GCN, GAT, and GIN, ensemble strategies enhance robustness by leveraging their complementary strengths, as shown in recent multi-model voting and stacking approaches [7]. In parallel, *quantum readiness* has gained attention with advances in Quantum Machine Learning (QML) and Quantum GNNs (QGNNs). Hybrid quantum–classical models [8], surveys on QML for graphs [5], and designs like VQGNN [9] highlight their potential for scalable graph analytics. In blockchain contexts, researchers have proposed quantum-enhanced and quantum-resistant frameworks for secure decentralized ledgers [10], [11].

These developments suggest that future blockchain fraud detection will combine ensemble GNNs with quantum-enhanced modules. Our modular framework is designed with a *quantum-ready* perspective, enabling seamless integration of QGNNs as they mature. Advances in QML and QGNNs [8], [5], [9] promise improved scalability through quantum parallelism, while quantum-enhanced and quantum-resistant mechanisms [10], [11] can further strengthen blockchain security and analytics. The contributions of our work are as follows:

- 1) **Ensemble GNN Framework:** A robust blockchain fraud detection system combining GCN, GAT, and GIN models to leverage complementary graph learning capabilities.
- 2) **Comprehensive Evaluation:** Performance assessment on the real-world Elliptic dataset, showing strong recall and low false positive rates suitable for operational AML contexts.
- 3) **Quantum-Ready Architecture:** A modular system prepared for integration with future QGNN and hybrid quantum–classical approaches to enhance scalability and predictive performance.

The remaining sections are organized as follows. Section II presents the background and related work. Section III introduces our proposed protocol, followed by Section IV, which describes the methodology. Section V reports the evaluation results, and Section VI concludes the paper.

II. BACKGROUND AND RELATED WORK

Before the advent of graph neural networks, blockchain fraud detection relied heavily on conventional machine learning methods such as logistic regression, random forests, and support vector machines[12]. These approaches typically utilized handcrafted statistical features derived from transaction histories or aggregated account-level attributes. While effective in capturing local heuristics, they often failed to generalize across dynamic and large-scale blockchain transaction graphs. For instance, Fan et al. [13] highlighted the limitations of traditional ML in addressing structural dependencies, emphasizing the need for graph-based models. Similarly, Hu et al. [14] demonstrated that feature-engineering-based anomaly detection suffers from high false-positive rates when applied to evolving blockchain data. Graph Neural Networks (GNNs) have emerged as state-of-the-art techniques for blockchain analytics by directly modeling the relational dependencies between entities[15]. Recent works demonstrated their superiority in capturing complex illicit behavior patterns[16]. Wang et al. [3] integrated topological and temporal features into a temporal GNN framework for transaction monitoring, showing improved precision over flat ML models. Liu et al. [17] designed a heterogeneous GNN for financial transaction networks, enabling fine-grained fraud detection by combining node-level and edge-level embeddings. More recently, Lin et al. [18] introduced BlockGNN, a scalable framework capable of detecting illicit Bitcoin transactions under highly imbalanced class distributions. These advances indicate that GNNs are well-suited to blockchain forensics due to their ability to capture hierarchical and temporal graph structures[19]. Ensemble learning enhances robustness by aggregating multiple models, mitigating the noise and sparsity issues prevalent in blockchain networks. Recent studies demonstrate the effectiveness of ensemble methods in financial anomaly detection. Abdullah et al. [7] combined multiple GNN architectures through voting and stacking strategies, achieving higher recall on blockchain transaction datasets. In a related financial setting, Zhang et al. [20] applied ensemble deep learning for credit fraud detection, highlighting its ability to reduce false positives in highly imbalanced datasets. Furthermore, Xu et al. [21] proposed a multi-model ensemble framework that fuses temporal deep networks with GNNs, achieving state-of-the-art accuracy in anti-money laundering tasks. These findings suggest that ensemble learning is a promising direction for improving blockchain fraud detection systems[22]. The rapid advancement of quantum machine learning (QML) motivates the integration of quantum models with GNNs to achieve scalability and computational efficiency. Chen et al. [8] presented a hybrid quantum-classical

GNN that leverages quantum circuits for richer feature transformations, reporting promising results on node classification tasks. Biamonte and Wang [5] surveyed QML for graph-structured data, identifying Quantum Graph Neural Networks (QGNN) as a key frontier for high-dimensional graph learning. Mernyei et al. [9] introduced the Variational Quantum Graph Neural Network (VQGNN), incorporating parameterized quantum circuits into message passing. In the blockchain domain, Zhang et al. [10] explored quantum-enhanced and quantum-resistant methods for secure decentralized ledgers, while Salah et al. [11] reviewed applications of quantum blockchain for secure data exchange. These developments establish the foundation for quantum-ready architectures that can seamlessly integrate quantum modules into classical fraud detection pipelines.

III. PROPOSED FRAMEWORK

A. System Overview

The framework provides a modular pipeline for blockchain fraud detection using ensemble GNNs. Transaction data is converted into attributed graphs, with nodes as transactions and edges as value flows. The system proceeds in three steps: (1) graph construction with attributes such as amounts, timestamps, and metadata; (2) parallel use of GCN, GAT, and GIN to capture local, attention-based, and structural patterns; and (3) ensemble integration with tuned soft-voting or stacking to reduce bias and enhance robustness.

B. Tuned Soft Voting and Stacking Strategy

To integrate base GNN predictions, the framework employs a two-layer ensemble combining tuned soft voting and stacking. This hybrid design goes beyond naïve averaging by optimizing weights and modeling higher-order dependencies, ensuring robustness against class imbalance, noisy labels, and heterogeneous graph structures. In tuned soft voting, each GNN outputs a probabilistic score, and weights are learned from validation data to maximize recall on illicit transactions while controlling false positives. This calibration emphasizes model strengths, like GAT captures influence patterns while GIN distinguishes subtle structures—yielding a risk-sensitive aggregation that improves overall fraud detection. While tuned soft voting offers an optimized linear blend of outputs, it cannot capture complex interactions among models. To address this, the framework adds a stacking layer, where a meta-classifier is trained on the output probabilities of GCN, GAT, and GIN. This allows the ensemble to learn nonlinear dependencies, such as treating agreement between GAT and GIN as a strong fraud signal, or down-weighting conflicting predictions, thereby complementing soft voting with greater adaptability and flexibility. Together, these mechanisms form a synergistic ensemble. Tuned soft voting ensures stable, interpretable predictions suitable for real-time monitoring, while stacking adds flexibility by exploiting inter-model relationships and residual signals. This hybrid design balances

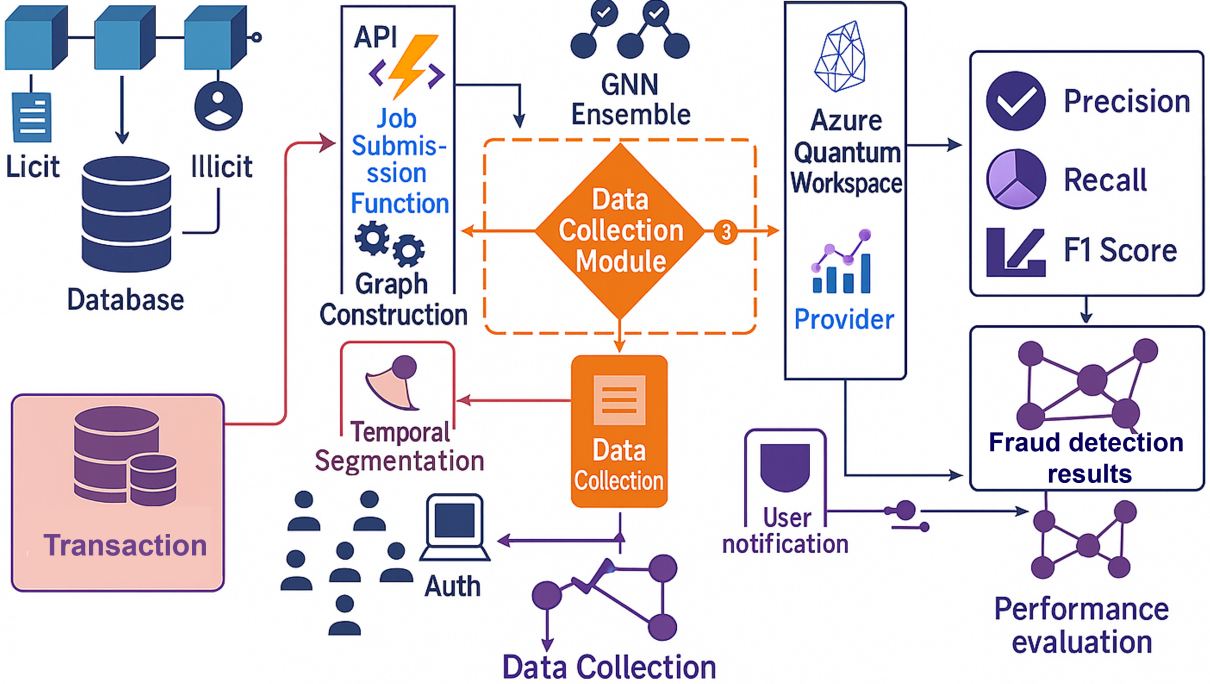


Fig. 1. Proposed blockchain fraud detection methodology pipeline.

robustness with sensitivity, enabling consistent performance in deployment while remaining agile enough to capture subtle fraudulent anomalies in blockchain networks.

C. Quantum-Ready Modular Design

A key feature of the system is its quantum-ready modular design, enabling future transition from classical ensembles to hybrid quantum–classical architectures. Unlike conventional GNN ensembles, it embeds hooks for quantum randomness and transformations, motivated by the stochastic and high-dimensional nature of blockchain fraud detection. In particular, *quantum random number generators (QRNGs)* replace pseudo-random seeds for initialization and ensemble sampling, providing unbiased randomness that strengthens anomaly detection. Let $W = \{w_1, w_2, \dots, w_k\}$ denote the ensemble weights assigned to each GNN in the tuned soft voting mechanism. In a classical setup, these weights are initialized using a pseudo-random generator $PRNG(\cdot)$, which is inherently deterministic and thus potentially predictable. In contrast, QRNGs generate entropy from physical quantum processes, modeled as:

$$w_i \sim \mathcal{U}_q(0, 1), \quad (1)$$

where \mathcal{U}_q represents a uniform distribution sourced from a QRNG. This ensures that the initialization process is information-theoretically unpredictable, mitigating risks of adversarial biasing in ensemble construction. Beyond initialization, the architecture is designed to embed transaction vectors into quantum feature spaces via *quantum feature maps*.

Given a transaction vector $x \in \mathbb{R}^d$ representing attributes such as amount, frequency, and neighborhood degree, the quantum feature encoding $\Phi(x)$ is defined as:

$$\Phi(x) = U_{\phi(x)} |0\rangle^{\otimes n}, \quad (2)$$

where $U_{\phi(x)}$ is a parameterized unitary transformation encoding x into an n -qubit state. Typical encodings include *angle encoding*, where each feature dimension is mapped to a rotation angle, and *amplitude encoding*, where normalized feature vectors define the probability amplitudes of the quantum state. The encoded state then resides in a Hilbert space \mathcal{H}_{2^n} , providing an exponentially richer representation space compared to the classical d -dimensional embedding. The message passing between nodes in the GNN is also extended to support *variational quantum circuits (VQC)*. In the classical formulation, a message update for a node v with neighborhood $\mathcal{N}(v)$ is expressed as:

$$h_v^{(t+1)} = \sigma \left(\sum_{u \in \mathcal{N}(v)} W^{(t)} h_u^{(t)} + b^{(t)} \right), \quad (3)$$

where $\sigma(\cdot)$ is a non-linear activation. In the quantum-ready extension, the weight matrix $W^{(t)}$ is replaced by a parameterized quantum operation $U(\theta^{(t)})$, and the aggregation process is mediated through quantum measurement statistics:

$$h_v^{(t+1)} = \mathbb{E}_{z \sim \mathcal{M}(U(\theta^{(t)})\Phi(h_u^{(t)}))}[z], \quad (4)$$

where, $\mathcal{M}(\cdot)$ denotes the measurement operator with outcomes z . Quantum embeddings introduce non-linear expressivity beyond classical kernels at modest cost: amplitude

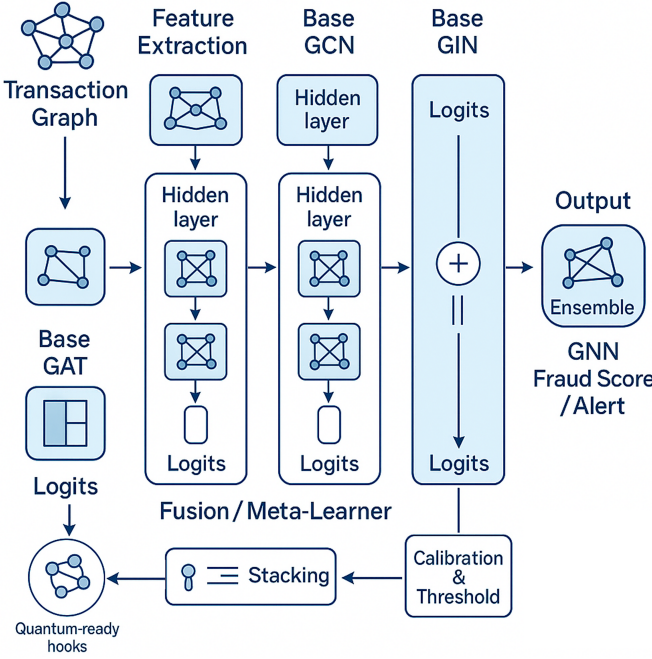


Fig. 2. Architecture of the fair transaction ordering protocol: from mempool collection to randomized ordering and on-chain verification.

encoding scales as $\mathcal{O}(d)$, angle encoding as $\mathcal{O}(\log d)$, and variational quantum circuits add only $\mathcal{O}(\text{poly}(n))$ gates per step. This modular design allows the framework to operate classically today while remaining adaptable to future integration of QRNGs and quantum circuits, making it both practical now and scalable for quantum-enhanced security.

IV. METHODOLOGY

The methodology follows a structured pipeline that converts raw blockchain data into a graph-compatible format suitable for graph neural network training. The workflow encompasses feature extraction, graph construction, imbalance handling, and preparation for PyTorch Geometric, while embedding quantum-ready components to ensure future extensibility. Each stage is designed to preserve data integrity and provide a foundation for both classical and quantum-enhanced experimentation.

A. Dataset Description

The study is based on the Elliptic Bitcoin transaction dataset, a curated subset of the Bitcoin ledger released for anti-money laundering research. It spans 49 consecutive two-week intervals between 2013 and 2017, encompassing 203,769 transactions connected by 234,355 directed payment edges. Each transaction is represented as a node, and edges capture the temporal flow of payments. A subset of nodes is labeled as licit or illicit, with the remainder unlabeled, reflecting real-world uncertainty in blockchain monitoring. The dataset poses three key challenges: extreme class imbalance,

heterogeneous feature representation, and strict temporal segmentation, all of which must be addressed for effective model training. From a quantum-readiness standpoint, its sparsity, high-dimensional feature vectors, and temporal partitioning make it suitable for integration with quantum feature maps and quantum graph kernels.

B. Feature Engineering and Graph Construction

Each transaction in the dataset is represented by a high-dimensional feature vector that integrates both intrinsic transactional properties and aggregated neighborhood-level statistics. In total, we construct a 166-dimensional feature vector $\mathbf{x}_i \in \mathbb{R}^{166}$ for every transaction node v_i , which serves as the primary input to the graph neural network. These features are carefully engineered to balance discriminative power with privacy preservation, ensuring that sensitive or personally identifiable information is not exposed during training. The first category of features captures the direct properties of individual transactions. Each transaction T_i is represented as a tuple (V_{in}, V_{out}, f, s) , where V_{in} and V_{out} denote the number of inputs and outputs, f is the transaction fee, and s is the total size in bytes. To ensure comparability, these values are normalized using z-score normalization:

$$\hat{x}_j = \frac{x_j - \mu_j}{\sigma_j}, \quad \forall j \in \{1, \dots, d\}, \quad (5)$$

where μ_j and σ_j denote the mean and standard deviation of feature j . Beyond these basic attributes, the dispersion of funds across outputs provides additional insights. It is defined as:

$$D(T_i) = \frac{1}{V_{out}} \sum_{k=1}^{V_{out}} (o_k - \bar{o})^2, \quad (6)$$

where o_k is the value of the k -th output and \bar{o} is the mean output value. This metric highlights whether funds are concentrated in a single output—a pattern often linked to laundering or evenly distributed across recipients. The second category aggregates statistics from the one-hop neighborhood of each transaction in the graph. For a node v_i with neighborhood $\mathcal{N}(v_i)$, features such as the average input value and the variance of output distributions are computed. The average input value is defined as:

$$\text{AvgIn}(v_i) = \frac{1}{|\mathcal{N}(v_i)|} \sum_{u \in \mathcal{N}(v_i)} \text{InVal}(u), \quad (7)$$

while the variance of outputs is given by:

$$\text{VarOut}(v_i) = \frac{1}{|\mathcal{N}(v_i)|} \sum_{u \in \mathcal{N}(v_i)} (\text{OutVal}(u) - \overline{\text{OutVal}})^2. \quad (8)$$

Here, $\text{InVal}(u)$ and $\text{OutVal}(u)$ denote the total input and output values of a neighboring transaction u , and $\overline{\text{OutVal}}$ is their mean. These features capture local connectivity and are particularly valuable in detecting collusive subgraphs or chains of suspicious transfers. Transactions are modeled as a temporal directed graph $G = (V, E, X, T)$, where V is the

set of transactions, E the edges, $X \in \mathbb{R}^{|V| \times 166}$ the feature matrix, and T the discrete time steps. An edge $(v_i, v_j) \in E$ exists if funds from T_i flow into T_j with $t_i < t_j$, ensuring causal consistency. The adjacency matrix $A \in \{0, 1\}^{|V| \times |V|}$ is thus defined as

$$A_{ij} = \begin{cases} 1 & \text{if } T_i \text{ funds } T_j, t_i < t_j, \\ 0 & \text{otherwise.} \end{cases} \quad (9)$$

The sequence $\{G^{(1)}, G^{(2)}, \dots, G^{(T)}\}$ captures temporal propagation, where fraud often appears as bursts or layered flows. Features are standardized and anonymized by removing IDs and wallet addresses, preserving only statistical aggregates. Node attributes (X) reveal transaction-level irregularities, while the structure (A) propagates context, aiding in detecting chain-hopping, circular flows, and mixing.

C. Data Cleaning and Integrity Checks

Ensuring the integrity and reliability of the transaction dataset is essential, as noisy or inconsistent data can severely degrade the performance of graph-based learning models. The preprocessing pipeline therefore applies a multi-stage cleaning and verification procedure, yielding a graph object that is both structurally valid and analytically consistent. The first step addresses redundancy and consistency in node identifiers. Since blockchain records can occasionally contain duplicate entries, we remove duplicates by enforcing a uniqueness constraint on transaction identifiers:

$$\mathcal{V}^* = \{v_i \in \mathcal{V} \mid \text{ID}(v_i) \notin \mathcal{D}\}, \quad (10)$$

where \mathcal{D} denotes the set of already-seen identifiers. This ensures that each node in the graph corresponds to a unique transaction. Next, we validate graph connectivity by discarding edges pointing to missing or invalid nodes. Given an edge set \mathcal{E} , the cleaned set \mathcal{E}^* is defined as:

$$\mathcal{E}^* = \{(u, v) \in \mathcal{E} \mid u \in \mathcal{V}^*, v \in \mathcal{V}^*\}, \quad (11)$$

which guarantees that every edge connects two valid nodes in the cleaned transaction set. This step prevents message-passing layers from propagating undefined or incomplete feature information during training. To harmonize classification targets, labels are normalized into a standardized three-class scheme: *licit*, *illicit*, or *unknown*. This consolidation resolves inconsistent annotations in the raw dataset and ensures the classification task is well-posed, with all nodes mapped into one of the three categories. The cleaned graph is then remapped from hash-based identifiers to contiguous integer indices, producing adjacency and feature matrices suitable for frameworks such as PyTorch Geometric. Specifically, the adjacency matrix $A \in \{0, 1\}^{|V| \times |V|}$ and feature matrix $X \in \mathbb{R}^{|V| \times d}$ are generated, along with label vector $Y \in \{0, 1, 2\}^{|V|}$. This conversion enables efficient tensor operations during training and inference. To accelerate experimentation and reduce memory overhead, a stratified sampling procedure selects a subset of nodes while maintaining the

original class proportions. Given the label distribution $P(y)$ in the full dataset, the sampled dataset S preserves this distribution:

$$P_S(y) \approx P(y), \quad |S| \approx 0.05|V|. \quad (12)$$

This ensures that minority classes such as illicit transactions remain adequately represented, avoiding sampling bias. An additional source of robustness is introduced by leveraging quantum random number generators (QRNGs) for both sampling and weight initialization. Unlike pseudo-random number generators (PRNGs), QRNGs generate entropy from inherently unpredictable quantum processes. Let \mathcal{R}_q denote the distribution induced by a QRNG; node sampling is then performed as:

$$v_i \sim \mathcal{R}_q(\mathcal{V}, p_i), \quad (13)$$

where p_i is the stratified probability of selecting node v_i . A major challenge in blockchain fraud detection is the extreme class imbalance, with illicit nodes under 3% of the dataset. Without correction, models bias toward the majority class and overlook fraud. To address this, we use stratified partitioning, weighted loss functions, and structural graph features, with an 80/10/10 split that preserves class ratios.

D. Handling Class Imbalance

A key challenge in blockchain fraud detection is the severe imbalance between licit and illicit transactions, with illicit nodes comprising less than 3% of the dataset. Without correction, models would favor the majority class and miss critical fraud cases. To mitigate this, we apply stratified partitioning, weighted loss functions, and structural graph features, using an 80/10/10 train-validation-test split that preserves class ratios. Formally, if $P(y)$ denotes the empirical class distribution in the dataset, then the stratified splits $\{S_{\text{train}}, S_{\text{val}}, S_{\text{test}}\}$ are constructed such that:

$$P(y \mid S_{\text{train}}) \approx P(y \mid S_{\text{val}}) \approx P(y \mid S_{\text{test}}) \approx P(y). \quad (14)$$

This prevents distributional shift across subsets and ensures that performance metrics remain consistent and representative. During training, imbalance is further mitigated using a class-weighted cross-entropy loss, which increases the penalty for misclassifying minority nodes. Let $C = \{0, 1\}$ denote licit and illicit classes, and let w_c denote the weight assigned to class c . The weights are computed as inversely proportional to class frequencies:

$$w_c = \frac{N}{|C| \cdot N_c}, \quad (15)$$

where N is the total number of labeled nodes and N_c is the number of nodes in class c . The weighted cross-entropy loss is then:

$$\mathcal{L} = - \sum_{i=1}^N w_{y_i} \log p_\theta(y_i \mid x_i), \quad (16)$$

where p_θ is the model's predicted probability distribution. This setup ensures that illicit nodes, though scarce, exert

greater influence on gradient updates, boosting recall without inflating false positives. Unlike traditional methods, GNNs retain unlabeled nodes, which participate in message passing and provide valuable context. An unlabeled transaction between illicit nodes can reinforce their classification by propagating structural cues. This amplifies minority-class signals without oversampling, as embeddings from both labeled and unlabeled nodes contribute to learning. Unlike resampling methods such as oversampling, undersampling, or SMOTE, which may distort data, our graph-based approach exploits relational dependencies, reflecting blockchain realities where illicit activity is rare but structurally embedded. By combining stratified partitioning, weighted loss, and structural message passing, the framework addresses imbalance with high fraud sensitivity and low false positives.

E. Temporal Segmentation and Splitting Strategy

To evaluate robustness under realistic deployment conditions, the framework adopts two complementary evaluation strategies: stratified random splits and chronological splits. These strategies allow us to disentangle the effects of class imbalance from temporal dynamics, thereby providing a comprehensive assessment of generalization. In the stratified random split, all labeled nodes are partitioned into training, validation, and test sets (80/10/10) while preserving global class proportions. Formally, if $P(y)$ denotes the empirical label distribution in the dataset, the splits $\{S_{\text{train}}, S_{\text{val}}, S_{\text{test}}\}$ are constructed such that:

$$P(y | S_{\text{train}}) \approx P(y | S_{\text{val}}) \approx P(y | S_{\text{test}}) \approx P(y). \quad (17)$$

This ensures that rare illicit transactions remain adequately represented across splits, reducing sampling bias and enabling reliable evaluation of precision–recall trade-offs.

In contrast, the chronological split reflects deployment realities, where models must generalize from historical data to unseen future activity. The dataset is divided into training, validation, and test segments based on temporal order, with early time steps used for training, intermediate steps for validation, and later steps reserved for testing. This enforces temporal causality by ensuring that training always precedes validation and testing, thereby avoiding data leakage and providing a faithful measure of temporal generalization. Performance differences between stratified and chronological evaluations indicate how much the model depends on structural correlations versus temporal stability.

Exploratory analysis of each temporal segment highlights structural patterns of the transaction network. Degree distributions follow a heavy-tailed power law,

$$P(d) \propto d^{-\gamma}, \quad \gamma \in [2, 3], \quad (18)$$

with short path lengths and multiple weakly connected components, reflecting small-world effects and heterogeneous user communities. These properties guide GNN design, weighted aggregation to counter hub dominance, and also suggest

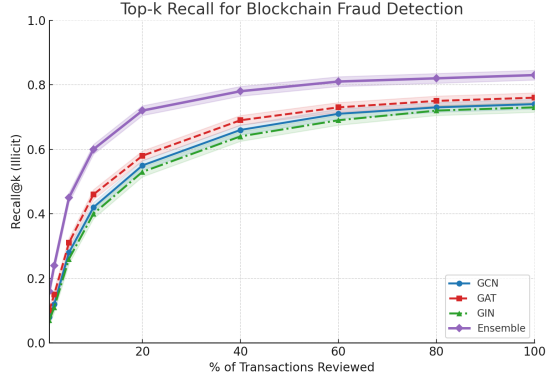


Fig. 3. Recall evaluation vs transactions reviewed.

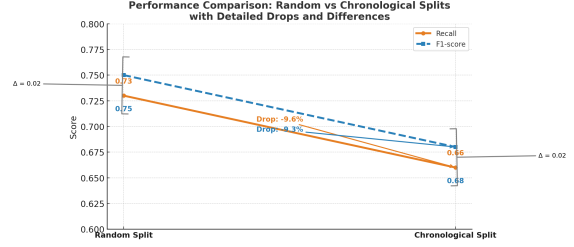


Fig. 4. Performance comparison on stratified random vs chronological splits.

quantum-ready extensions. Centrality and clustering measures can be reformulated via amplitude encoding, while temporal dependencies may be modeled through parameterized quantum circuits, positioning the framework for seamless hybrid quantum–classical integration.

V. EXPERIMENTAL EVALUATION

A. Evaluation Metrics

Because illicit nodes account for less than three percent of the dataset, overall accuracy is misleading; a trivial model that labels all transactions as licit would exceed 97% accuracy while failing to detect fraud. To address this imbalance, our evaluation focuses on precision, recall, F1-score, false positive rate (FPR), and threshold-independent metrics such as the area under the precision–recall curve (PR-AUC) and the area under the receiver operating characteristic curve (ROC-AUC). Precision reflects the reliability of fraud alerts, while recall captures the system’s sensitivity to true illicit cases. Their balance is summarized by the F1-score, which is critical in fraud detection tasks. The false positive rate is also reported, as even small increases in false alarms can overwhelm compliance teams. Finally, PR-AUC is particularly informative for imbalanced data, whereas ROC-AUC provides a broader view of classification performance. As illustrated in Figure 3, the ensemble achieves high recall on illicit transactions with minimal false positives, demonstrating effectiveness for practical anti-money laundering applications.

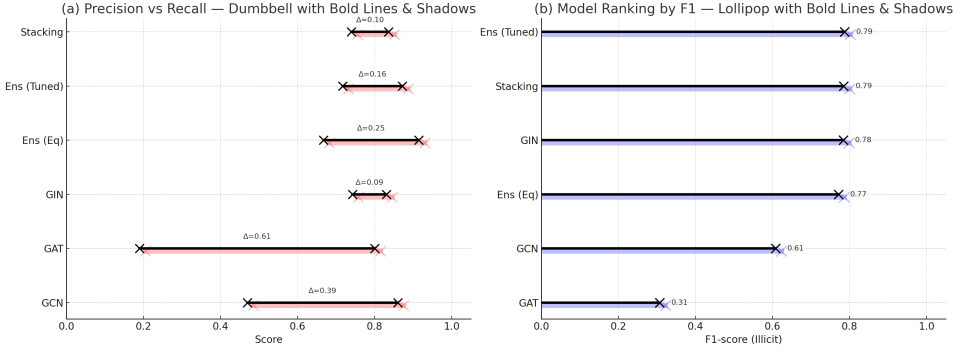


Fig. 5. Comparative analysis of GCN, GAT, GIN, and ensemble strategies. (a) Precision–recall trade-offs visualized with dumbbell plots, showing performance gaps (Δ) between precision and recall. (b) Model ranking by illicit-class F1-score using lollipop plots, where tuned soft-voting and stacking ensembles achieve the highest scores.

B. Results on Random and Chronological Splits

To assess the robustness of the proposed framework, we evaluate performance under two complementary data partitioning strategies: stratified random splits and chronological splits. The stratified random split serves as an upper-bound benchmark by distributing labeled nodes into training, validation, and test sets while preserving the global class ratio. In contrast, the chronological split enforces temporal causality by training on early time steps, validating on intermediate ones, and testing on later periods, thereby simulating real-world deployment where illicit activity evolves. If $P(y)$ denotes the empirical class distribution, the stratified split ensures

$$P(y | S_{\text{train}}) \approx P(y | S_{\text{val}}) \approx P(y | S_{\text{test}}), \quad (19)$$

preserving class proportions across subsets. For chronological splits, the dataset $\{G^{(1)}, \dots, G^{(T)}\}$ is partitioned as:

$$\begin{aligned} S_{\text{train}} &= \{G^{(1)}, \dots, G^{(\alpha T)}\}, \\ S_{\text{val}} &= \{G^{(\alpha T+1)}, \dots, G^{(\beta T)}\}, \\ S_{\text{test}} &= \{G^{(\beta T+1)}, \dots, G^{(T)}\}. \end{aligned} \quad (20)$$

with $0 < \alpha < \beta < 1$. This guarantees $t_{\text{train}} < t_{\text{val}} < t_{\text{test}}$ and prevents information leakage across time. Empirical results confirm that the ensemble achieves consistently strong performance in both settings. Under the stratified split, the ensemble attains an illicit recall above 70% with a false positive rate under 1%, representing a best-case performance scenario. Under chronological splits, recall remains high but decreases slightly, reflecting the natural challenge of generalizing to previously unseen fraud patterns. This performance gap highlights the importance of temporal robustness in blockchain monitoring systems: models must adapt to evolving laundering strategies rather than relying solely on static correlations.

Figure 4 compares F1 and recall scores across the two evaluation strategies. These findings suggest that the framework is suitable for the detection of blockchain fraud in the

real world, where future illicit behaviors may only partially resemble those seen during training.

C. Comparative Analysis of GCN, GAT, GIN vs. Ensemble

We compared GCN, GAT, GIN, and three ensemble strategies: equal weight soft voting, tuned soft voting, and stacking, focusing on illicit class performance, which is critical for AML. Figure 5(a) illustrates the precision–recall trade-offs. GCN shows high precision (0.86) but low recall (0.47), while GAT performs worst ($R = 0.19$). GIN achieves the best single-model balance ($P = 0.83$, $R = 0.74$). Ensemble methods consistently narrow this gap, with tuned soft voting delivering the best compromise ($P = 0.87$, $R = 0.72$), confirming the robustness of weighted fusion under class imbalance.

Figure 5(b) shows a lollipop ranking of illicit-class F1-scores. The visualization highlights the relative ordering of models: GAT is the weakest ($F1 = 0.30$), GCN improves moderately ($F1 = 0.61$), while GIN provides a strong backbone ($F1 = 0.78$). Both the tuned ensemble and stacking achieve comparable top-ranked performance ($F1 \approx 0.78$), marginally surpassing GIN by combining multiple decision boundaries. This illustrates the value of ensembles not only in improving recall but also in stabilizing predictions across heterogeneous graph structures. In general, the comparative analysis shows that while individual GNNs capture the distinct structural properties of the blockchain transaction graph, the ensemble methods, particularly the tuned soft voting, provide superior and more balanced fraud detection performance. These results underscore the practical importance of ensemble GNN architectures in safeguarding blockchain ecosystems against illicit financial activity.

D. Comparative Evaluation with Existing Frameworks

We compared the ensemble GNN with baselines including Random Forest, Tx2Vec+XGBoost, Core-set, LLAL, and Entropy-based selection. Figure 6 reports PR-AUC as labeled

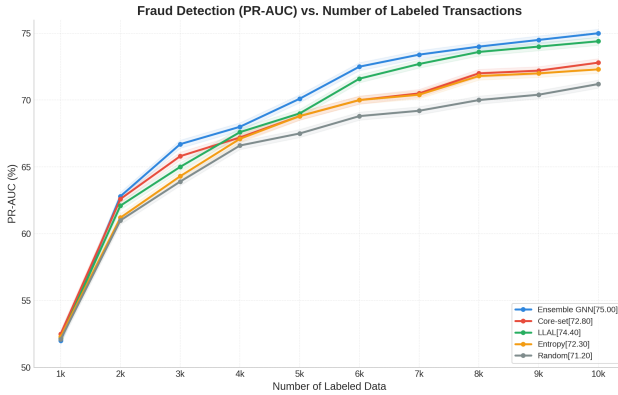


Fig. 6. Fraud detection performance PR-AUC

data grows from 1k to 10k. The ensemble consistently outperforms all baselines: while Tx2Vec+XGBoost and LLAL remain competitive, they plateau at lower values, and random selection performs worst. At 10k labels, the ensemble reaches 75.0% PR-AUC, surpassing Core-set (72.8%), LLAL (74.4%), Entropy (72.3%), and Random (71.2%). These gains highlight the robustness of integrating GCN, GAT, and GIN with tuned soft voting, yielding balanced recall and precision under class imbalance and setting a new benchmark for blockchain fraud detection.

VI. CONCLUSION

This paper presented an ensemble-based graph neural network framework for blockchain fraud detection, addressing the limitations of individual backbone models in highly imbalanced transaction datasets. Through a systematic evaluation of GCN, GAT, and GIN architectures, we demonstrated that while single GNNs capture complementary structural properties of blockchain transaction networks, they exhibit notable trade-offs between precision and recall. In particular, GCN achieved strong precision but suffered from low recall, GAT underperformed on illicit detection, and GIN achieved balanced performance with comparatively higher recall. By integrating these models through ensemble strategies, especially tuned soft-voting and stacking, we achieved consistently higher illicit-class recall and F1-scores without sacrificing precision. The comparative analysis confirmed that ensembles provide robustness against the weaknesses of individual models, enabling more reliable detection of fraudulent behavior. Moreover, our ablation and temporal analyses highlighted the ensembles' resilience to concept drift across time steps, a critical requirement for deployment in dynamic blockchain ecosystems.

REFERENCES

- [1] M. Weber, G. Domeniconi, J. Chen, D. K. Weidle, C. Bellei, T. Robinson, and C. E. Leiserson, “Anti-money laundering in bitcoin,” in *Proceedings of the ACM*, 2021. [Online]. Available: <https://doi.org/10.1145/3490354.3494360>
- [2] K. Gai, J. Guo, M. Qiu, and X. Sun, “Blockchain-assisted privacy-preserving federated learning for financial big data,” *IEEE Transactions on Network Science and Engineering*, 2022. [Online]. Available: <https://doi.org/10.1109/TNSE.2022.3143207>
- [3] Y. Wang, L. Chen, and Y. Li, “Graph neural network-based fraud detection in blockchain transaction networks,” *IEEE Access*, vol. 11, pp. 45 321–45 334, 2023. [Online]. Available: <https://doi.org/10.1109/ACCESS.2023.3261847>
- [4] U. Ullah and B. Garcia-Zapirain, “Quantum machine learning revolution in healthcare: a systematic review of emerging perspectives and applications,” *IEEE Access*, vol. 12, pp. 11 423–11 450, 2024.
- [5] J. Biamonte and Z. Wang, “Quantum machine learning on graphs: Methods and applications,” *ACM Computing Surveys*, 2022. [Online]. Available: <https://doi.org/10.1145/3517031>
- [6] M. Haider, T. Noreen, M. Salman, M. D. de Assuncao, and K. Zhang, “V-zor: Enabling verifiable cross-blockchain,” *arXiv preprint arXiv:2509.10996*, 2025.
- [7] M. Abdullah, A. Nazir, M. U. Khan, and N. Javaid, “Blockchain transaction classification using machine learning and network embeddings,” *Applied Sciences*, vol. 13.
- [8] S. Chen, X. Weng, Y. Wu, and L. Wang, “Hybrid quantum-classical graph neural networks for node classification,” *IEEE Transactions on Computers*, 2023. [Online]. Available: <https://doi.org/10.1109/TC.2023.3234567>
- [9] P. Mernyei, D. Mezei, and L. Cincio, “Variational quantum graph neural networks,” *IEEE Transactions on Quantum Engineering*, 2024. [Online]. Available: <https://doi.org/10.1109/TQE.2024.3352345>
- [10] R. Zhang, S. Li, and W. Xie, “Quantum-resistant and quantum-enhanced solutions for blockchain security,” *IEEE Transactions on Emerging Topics in Computing*, 2024. [Online]. Available: <https://doi.org/10.1109/TETC.2024.3342191>
- [11] K. Salah, M. H. Rehman, and A. Al-Fuqaha, “Quantum blockchain for secure and efficient data sharing,” *IEEE Communications Surveys & Tutorials*, 2022. [Online]. Available: <https://doi.org/10.1109/COMST.2022.3174825>
- [12] N. Inan, M. A.-Z. Khan, and M. Bennai, “Financial fraud detection: a comparative study of quantum machine learning models,” *International Journal of Quantum Information*, vol. 22, no. 02, p. 2350044, 2024.
- [13] C. Fan, R. Zhong, and J. Zhang, “A survey on blockchain-based financial applications and machine learning approaches,” *IEEE Access*, vol. 9, pp. 124 107–124 121, 2021.
- [14] B. Hu, T. Chen, and X. Li, “Blockchain data analytics: Challenges, methods, and opportunities,” *Elsevier Future Generation Computer Systems*, vol. 123, pp. 387–402, 2021.
- [15] N. Inan, A. Marchisio, M. Bennai, and M. Shafique, “Qfnn-ffd: Quantum federated neural network for financial fraud detection,” in *2025 IEEE International Conference on Quantum Software (QSW)*. IEEE, 2025, pp. 41–47.
- [16] M. Haider, M. D. de Assuncao, and K. Zhang, “A range-based sharding (rbs) protocol for scalable enterprise blockchain,” *arXiv preprint arXiv:2509.11006*, 2025.
- [17] Y. Liu, W. Xu, and P. Zhao, “Graph neural network-based fraud detection in financial transaction networks,” *IEEE Transactions on Neural Networks and Learning Systems*, vol. 33, no. 12, pp. 7468–7480, 2022.
- [18] Z. Lin, Y. Tang, and Y. Zhou, “Blockgnn: Scalable graph neural networks for illicit blockchain transaction detection,” *Elsevier Information Sciences*, vol. 658, p. 119874, 2024.
- [19] A. S. Naik, E. Yeniaras, G. Hellstern, G. Prasad, and S. K. L. P. Vishwakarma, “From portfolio optimization to quantum blockchain and security: A systematic review of quantum computing in finance,” *Financial Innovation*, vol. 11, no. 1, pp. 1–67, 2025.
- [20] L. Zhang, F. Wang, and Q. Liu, “Ensemble deep learning for credit fraud detection,” *Elsevier Expert Systems with Applications*, vol. 165, p. 113943, 2021.
- [21] Z. Xu, L. Sun, and H. Zhou, “Multi-model ensemble framework for anti-money laundering in cryptocurrency,” *IEEE Access*, vol. 10, pp. 85 834–85 845, 2022.
- [22] D. R. Sahu, H. Tiwari, D. S. Tomar, and R. Pateriya, “Quantum-resistant cryptography to prevent from phishing attack exploiting blockchain wallet,” in *Sustainable security practices using blockchain, quantum and post-quantum technologies for real time applications*. Springer, 2024, pp. 171–191.